Advancements in Machine Learning for Early Detection of Neurological Disorders: Focus on MRI-Based Diagnostics

Zaituna Assyl, Bachelor of Science

Submitted in fulfillment of the requirements for the degree of a Master of Science in Biomedical Engineering

School of Engineering and Digital Sciences
Department of Chemical and Materials Engineering
Nazarbayev University

53 Kabanbay Batyr Avenue,
Nur-Sultan, Kazakhstan, 010000

Lead Supervisor: Associate Professor Cevat Erisken

Co-supervisor: Associate Professor Dhawal Shah

April, 2025

DECLARATION

Under the guidance of Professor Cevat Erisken from Nazarbayev University, I hereby declare that my thesis "*Machine Learning for early detection of neurological disorders*" is the result of my own work.

I confirm that no other degree or diploma has been awarded for the full or partial submission of this dissertation to any other school. All references to sources, reference materials and data are duly confirmed and quoted in the text.

I affirm that this dissertation meets the academic and ethical requirements of Nazarbayev University. Any violation of these standards, including plagiarism and deception, will be subject to disciplinary action.

The project entitled “Advances in Machine Learning for Early detection of neurological disorders: Focus on MRI-based diagnosis” was reviewed by Nazarbayev University Institutional Research Ethics Committee (NU IREC) and approved on April 16, 2025 (Approval No 1063/16042025).

Name: Zaituna Assyl

Data: April, 2025

Acknowledgements

I wish to express my deepest gratitude to my supervisor, Professor Cevat Erisken, for their constant guidance, valuable advice and support throughout the work on this thesis. Their experience, support, and meaningful feedback played an important role in shaping this study and overcoming the difficulties I faced during the research.

I would also like to sincerely thank the faculty and staff of the Department of Chemical and Materials Engineering at Nazarbayev University for providing me with the necessary knowledge, resources and academic environment, which greatly contributed to my learning and research experience.

Special thanks to my family and friends for their unconditional support, patience, and motivation throughout my Master's degree program. Their support and understanding have been a constant source of strength during this difficult but rewarding process.

Finally, I take this opportunity to thank the authors and co-authors of the publicly available datasets used in this study. Without their efforts to share valuable medical imaging data, this study would not have been possible.

Table of Contents

List of abbreviations

ML	Machine Learning
MRI	Magnetic resonance imaging
CNN	Convolutional neural networks
NLD	Neurological disorders
AD	Alzheimer's disease
PD	Parkinson’s disease
SZ	Schizophrenia
MMSE	Mini-Mental State Examination
PET	Positron emission tomography
CT	Computed tomography
RBD	Sleep behavior disorder
REM	Rapid Eye Movement
HC	Health Control
MMSE	Mini-mental State Examination
MCI	Mild Cognitive Impairment
NF1	Neurofibromin 1
MAPK	Mitogen-Activated Protein Kinase
2HG	2-hydroxyglutarate
IDH	Isocitrate Dehydrogenase
SVM	Support Vector Machines
CSF	Cerebrospinal Fluid
CRR Model	Cox Ross Rubinstein Model
ROI	Region of Interest
LoG	Laplacian of Gaussian

List of Figures and Tables

Abstract

Globally, the most frequent reasons for disability are brain diseases such multiple sclerosis, Brain Tumor, and Alzheimer's disease. In an effort to reduce the progression of the disease and improve patient outcomes, early identification is essential. Magnetic resonance imaging (MRI) which is a non-invasive imaging method provides important information on anatomical and functional alterations in the brain, making it a potentially useful tool for early diagnosis. The execution of machine learning (ML) algorithms to MRI data for the early identification of neurological illnesses is examined in this thesis.

The results show that CNN-based models perform better than other strategies in detecting early illness signs, yielding notable gains in accuracy when compared to conventional diagnostic techniques. The thesis also discusses problems including class imbalance, data heterogeneity, and the interpretability of machine learning models, offering solutions.

This study demonstrates the promise for automated, scalable, and precise diagnostic tools to support physicians in the early identification and intervention of neurological illnesses by fusing machine learning with MRI data. Expanding datasets, integrating multimodal data, and enhancing model generalizability to actual clinical settings will be the main goals of future research.

Keywords: Machine learning, Neurological Diseases, Brain MRI, CNN, Deep Learning.

CHAPTER 1 - (INTRODUCTION)

1.1. Neurological Disorders

Neurological health threats rank as a leading global health risk because they generate substantial consequences for both human patients and health services worldwide. AD and PD and SZ represent the three leading neurological disorders which manifest through impairments of regular brain functioning [1]. The advanced neurological condition destroys brain cells while degenerating cognitive functions and memory abilities so patients gradually lose the ability to perform basic activities. The cognitive deterioration from the disease ends in dementia. Neurodegenerative dementia starts with subtle decline yet continually worsens throughout its development course [8]. The three progressive stages of Alzheimer's disease start with extremely mild symptoms followed by mild symptoms and then progress to moderate symptoms. Medical professionals struggle to reliably diagnose Alzheimer's disease when patients have not reached that condition yet. A precise assessment of AD needs both physical and neurological tests together with the Mini-Mental State Examination (MMSE) and a detailed medical history. Medical professionals have begun utilizing Brain MRI tests to detect Alzheimer's disease among patients. The disease affects both cerebral cortex and hippocampus regions of the brain through atrophy while expanding ventricular cavities [14].

1.1.1. Early Detection

To slow the progression of neurological illnesses or, ideally, stop them completely, early detection is crucial. Deep learning-based analytical approaches and sophisticated neuroimaging techniques as well as positron emission tomography (PET), computed tomography (CT), and magnetic resonance imaging (MRI) have been created. Certain resources aid in the early diagnosis of particular conditions and aid in the development of successful treatment strategies.

Scientists have created a number of computer-aided diagnostic methods to accurately diagnose diseases. The 1970s to 1990s saw the development of expert systems, and starting in the 1990s, supervised models [3]. Machine learning (ML) has been successfully used in several

disciplines over the past ten years, particularly in image analysis and illness identification [4, 5]. Given the favorable outcome of deep learning computer vision algorithms, neuroimaging researchers have worked to identify these neurological conditions from MRI scans using deep learning-based methods.

Researchers have achieved important progress in both brain injury evaluation and brain anatomy examination through MRI monitoring since the past few years [16]. The medical procedure MRI demonstrates its ability to detect neurological conditions according to research [17]. Medical professionals use time-series brain MRI segmentation to analyze structural brain modifications at different assessment periods. The exact identification and classification of injured tissue together with adjacent healthy structures form the basis of proper medical diagnosis. The diagnosis requires significant data accumulation to reach sufficient accuracy. An automated segmentation method must advance because it delivers reliable and precise results. Recently clinicians have used computer-based methods to analyze large datasets for enhancing accurate and high-quality medical diagnoses through segmentation and imaging combined with MRI recording.

1.1.2. Selecting the most effective approach

Research findings play a vital role in selecting appropriate methods for specific datasets since this field has gained more interest alongside the rising number of MRI scan analysis procedures [6]. Recent advancements in mental health research have been driven by the integration of big data technologies and machine learning approaches [7]. The majority of methodologies utilize manual operations to build and obtain features from MRI data. Using logistic regression along with support vector methods enables manual functions to work more efficiently for classification purposes [1]. Today's greatest deep learning algorithms successfully process genuine world photo compositions. To avoid model overfitting the network demands massive amounts of equally distributed training data as recommended through these prototypes [1].

Measuring changes in brain structures over time involves segmenting MRI images taken at different points in time. In addition, accurate identification and localization of abnormal tissues, as well as the healthy areas surrounding them, are crucial for accurate diagnosis, surgery planning, and postoperative evaluation. Considerable progresses have been made in the growth of classical

machine learning methods for segmenting both normal brain tissues and abnormal tissues (such as tumors) in MRI images [18].

1.2. Hypothesis

CNNs function as deep learning models that investigate brain MRI images to speed up medical identification and precise neurological condition classifications. The model will achieve outstanding multi-class diagnostic capabilities which separate between Alzheimer's disease and glioma and meningioma along with healthy brain structures and brain cases with no tumors.

Research shows the model achieves exceptional performance in detecting brain tumors since their characteristics are evident on MRI results. Early-stage Alzheimer's disease classification poses a major problem because its brain structural changes occur subtly during progressive development. Directional diagnosis support with clinical choices in neurological disease detection can be achieved when the proposed deep learning model analyzes a broad dataset through advanced image processing algorithms.

1.3. Aim and objectives

The main objective of this research is to create and test an AI-based classification tool that identifies neurological disorders through brain MRI analysis while focusing on Alzheimer's disease and glioma and meningioma diagnosis. Paving the way toward our objective involved obtaining a complete dataset from public resources which contained five distinct categories namely dementia and glioma, meningioma and dementia-free, tumor-free images. A preprocessing stage included resizing and normalization and scaling up of images to enhance training performance in the model. Subsequently, a convolutional neural network was developed to automatically analyze image features for classification tasks. Performance evaluation of the model relied on assessing accuracy alongside precision and memorability and F1 score. The model's capability to distinguish between Alzheimer's disease brain images and healthy brain images became the special focus of evaluation since this distinction proves challenging for medical experts. The research investigated both the advantages and limitations of this model before proposing strategies to enhance deep learning applications in neurological diagnosis.

CHAPTER 2 - (MATERIALS AND METHODS)

2.1. An outline of deep learning methodology

The development of machine learning frameworks especially deep learning enables model creation to draw features with high dimensions from data collections. Image segmentation functions within its own field of image processing to separate graphical content into separate meaningful parts. The article in reference 9 explains image segmentation methods through a process of semantic element segmentation of pictures. Image-processing within the medical field demands localization service to detect postoperative medical abnormalities like tumors and specific organs according to [9]. The deep learning methodology goes beyond traditional features since these models extract complicated data patterns by themselves through automated learning strategies. The processing of big datasets allows these systems to produce outstanding accuracy levels and strong generalization abilities during the analysis and segmentation of brain regions in MRI brain images. Surveillance operations gain significant worth from the practice of division.

Machine learning contains deep learning as a subset that allows models to find different features automatically at all dataset depths. Multiple-tier neural networks operate in pattern recognition tasks that deal with raw input images according to [18]. Standard machine learning works with human-generated features during data processing yet deep learning automatically discovers multiple complex patterns by learning features automatically. Large datasets enable their processing capabilities to reach generalization in their output while maintaining perfect accuracy.

Image segmentation belongs to the core processing techniques of image processing because it transforms images into meaningful sections. The segmentation process allows medical practitioners to establish unambiguous contours between essential imaging features such as organs as well as tumors and brain regions. The analysis of brain areas in MRI scans reaches higher performance levels with deep learning approaches compared to standard tools because they deliver superior results in these applications.

The combination of abnormality localization and postoperative structure detection achieves effective diagnosis planning and postoperative assessment through deep learning models [9].

In the context of image processing, one key technique is image segmentation, which divides an image into two or more meaningful parts. Segmentation allows for the delineation of borders between distinct semantic objects within an image, such as tumors, organs, or brain regions, and is particularly important in medical imaging. In this domain, deep learning models have showed superior performance in segmenting and analyzing brain regions in MRI scans, providing more accurate results compared to traditional methods.

Additionally, deep learning models have proven effective in applications such as localizing abnormalities (e.g., tumors) and identifying structures of interest after surgeries, which are crucial for diagnosis, surgical planning, and postoperative assessment [9].

2.1.1 Convolutional neural network (CNN)

MRI data can be applied to detect neurological problems early thanks in large part to Convolutional Neural Networks (CNNs). CNNs are an extremely effective class of deep learning models for brain imaging applications because they are made to process and interpret structural and spatial patterns in imaging data. Convolutional Neural Networks, sometimes referred to as ConvNets, typically take an input image and use biases and learnable weights to discriminate between different parts of the image. In at least one of its layers, CNN substitutes a convolution process for basic matrix multiplication. Its primary application is in unstructured datasets, such as images and videos [6]. CNNs automatically learn hierarchical aspects from MRI data, including structural abnormalities, brain volume, and cortical thickness. These traits are suggestive of early neurological alterations in conditions like Brain Tumor or Alzheimer's disease. Fully linked layers, pooling layers, and convolutional layers make up CNN structures.

Typically, a feature map is produced by stacking numerous convolutional and pooling layers one after the other. The ensuing map is then input into the layer that is entirely connected. The convolutional layer applies a filter to the image represented by pixel matrices of a predetermined size of n×n. By browsing the complete picture matrix and going over the pixel matrices, the filter is applied. Pivot on the kind of filter used, certain aspects of the picture become

visible. The subsampling procedure is used to decrease the spatial dimension's size in the pooling layer.

In this sense, combining layers avoids overfitting and also simplifies calculations. The maximum merge selects the window's highest pixel, whereas the average merge uses the average pixel value of the window. Then the fully connected layer, could be multi-layered perceptrons, classifies the data based on the feature map containing the extracted features [12].

2.1.2. Techniques for pre-processing data

To improve the experimental data's integrity and get them ready for additional statistical analysis, the pre-processing stage is crucial. Various MRI scan modalities obtained from various sources are prone to a wide variety of noise, such as stirring, median signal strength, and spatial affection, which must be eliminated from the data to guarantee accurate interpretation [6].

2.2. Determination of neurological conditions

2.2.1. Alzheimer's disease

Early identification of AD is becoming more and more dependent on the detection of physical alterations in the brain, which supplement clinical evaluations. To quantify the degenerative brain alterations associated with Alzheimer's disease, researchers have been focusing their efforts on neuroimaging techniques.

The gradual decline of thinking and behavior and memory functions in Alzheimer's disease creates challenges for daily execution of tasks. The main indicators of AD pathology include tau tangles with beta-amyloid plaques because these impair neuronal signaling and result in neuron death [21]. The decline in cognitive abilities happens due to these changes that start in the hippocampus which is responsible for memory formation before spreading to other brain regions [22]. The research indicates that projections for Alzheimer's disease in Americans aged 65 and older point to 6.9 million people during 2024 while 73% of these cases will affect individuals over 75 years old (Fig. 1) [23].

Due to the fact that aging is a major risk factor for developing Alzheimer's dementia, both new and current cases of the disease will increase rapidly along with the number and proportion of older Americans (Fig.2).

It is estimated that by 2060, 13.8 million people aged 65 and over will have Alzheimer's dementia unless new treatments are developed to prevent or treat the disease [24].

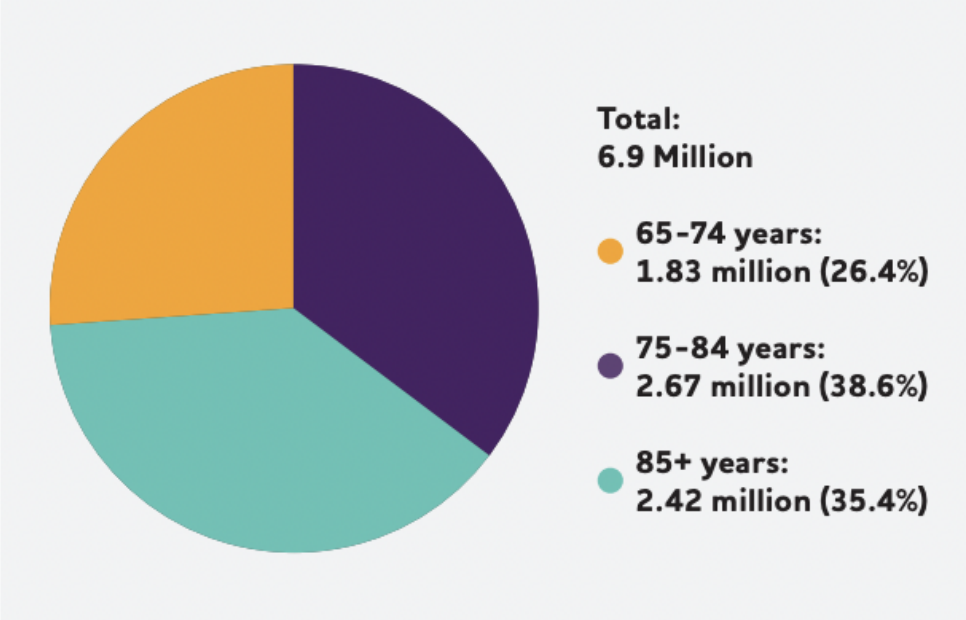

Figure 1. Ages and Numbers of Individuals with Alzheimer's Disease Aged 65 an Over, 2024

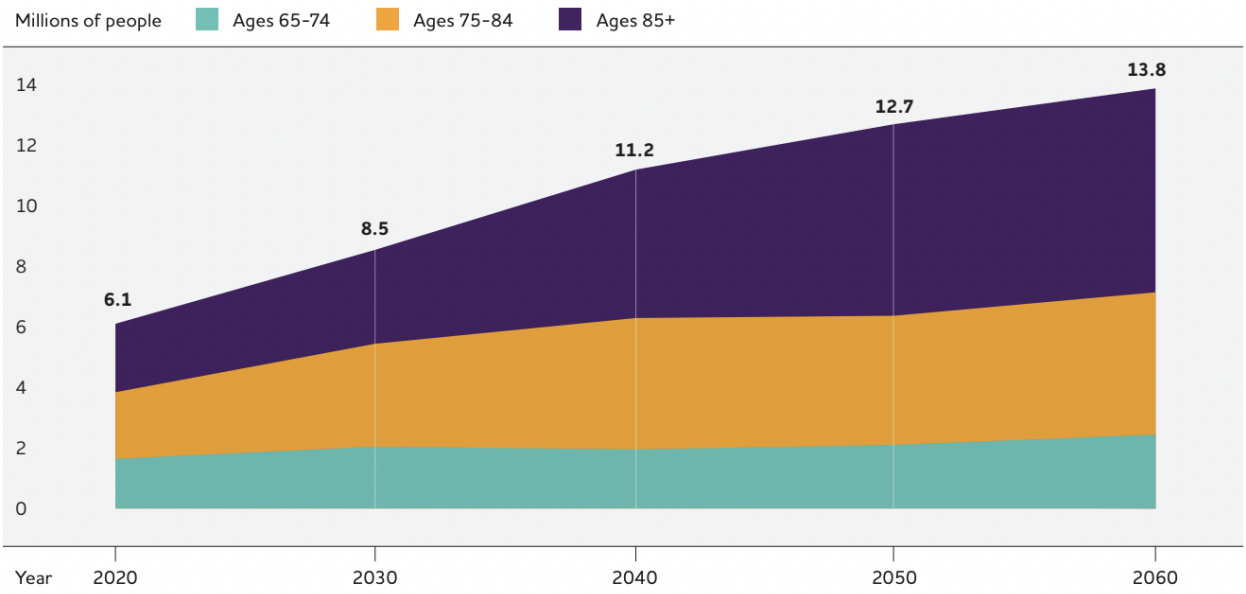

Figure 2. The estimated number of Americans 65 and older who have Alzheimer's disease, both overall and by age, from 2020 to 2060.

Studies indicate that Alzheimer's disease (AD) affects less than half of dementia patients because most dementia cases exist as a mixed form. The development of Alzheimer's disease leads to dementia in 60 to 80% of affected patients [25]. The risk of developing dementia-related conditions increases by double frequency every 6.3 years starting from an initial rate of 3.9 per 1,000 individuals aged 60 to 90 years until reaching 104.8 per 1,000 people older than 90 years making age the main precocious factor for Alzheimer Disease [26].

A moderate or severe atrophic change affects the cerebral cortex during Alzheimer's disease manifestations while showing most extensive damage in the limbic and multimodal associative brain regions. The brain atrophy shows clear signs in the frontal and temporal lobes since it causes gyri reduction and furrows to expand. During early stages combined with intermediate phases of the disease the primary motor area along with the sensory cortex typically remain unchanged although structural variations can still occur [27].

According to recent functional and structural imaging studies, atrophy of the posterior brain regions, especially the precuneus and posterior cingulate gyrus, also significantly affects patients with Alzheimer's Disease (Fig. 3) [28, 29]. It is becoming increasingly clear that these areas are early targets of neurodegeneration in AD.

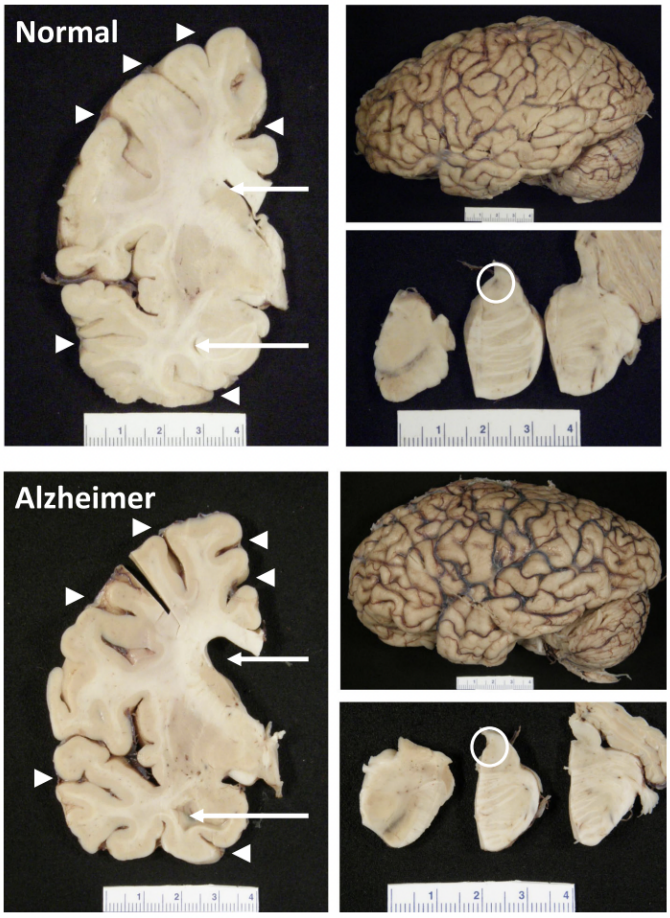

Figure 3. Gross Anatomy of Alzheimer's Brain [30].

Early detection of Alzheimer's disease is crucial for several reasons. First, prompt interventions made possible by early diagnosis may benefit patients' quality of life by delaying the onset of symptoms. To identify Alzheimer's disease early on, researchers have created and improved neuropsychological assessments, neuroimaging methods, blood and cerebrospinal fluid biomarkers, and even artificial intelligence tools.

The authors [13] in their study, they develop a learning algorithm that can distinguish between healthy and sick brains using MRI scans as input. They looked at a subclass of deep artificial neural networks, more especially a convolutional neural network and sparse autoencoder combination. The primary invention of the technique is the use of 3D convolutions on the entire MRI picture, which in our tests performs better than 2D convolutions on slices. They presented the classification findings from three binary classifiers (AD vs. HC, AD vs. MCI, and MCI vs. HC) and a three-way classifier (HC vs. AD vs. MCI).

According to recent studies Yigit and Isik (2020), They employed T1-weighted MR image samples in their investigation to differentiate between people in good health, Alzheimer's disease patients, and people with mild cognitive disablement. While the other set of MR data was utilized for testing, the first set was used for training. MR slices were chosen in three dimensions and then downsized to two dimensions after the image data was obtained. A strategy for data augmentation was used because the quantity of images for various projections was not equal.

A few preprocessing techniques were used prior to the photographs being used as model input. CNN models were developed with varying numbers of layers and used to categorize the various forms of Alzheimer's disease. Performance was evaluated using the suggested model's diagnostic power.

2.2.2. Glioma

The significant morbidity and death rate of brain tumors is a result of their location and frequently locally invasive growth. Metastases from malignancies outside the central nervous system, which are five to ten times more prevalent than original brain tumors, account for the majority of neoplastic brain lesions [31]. The two most prevalent forms of primary brain tumors are gliomas and meningiomas (Fig. 4) [32, 33]. Gliomas account for almost 30% of all primary brain tumors and are responsible for approximately 80% of deaths associated with malignant brain tumors. Histologically, this diverse group of tumors is classified based on their morphological similarity to the types of neuroglial cells present in the normal brain, including astrocytomas, oligodendrogliomas, mixed oligoastrocytic gliomas, and ependymomas. It is generally believed that these tumors originate from neuroglial stem cells or progenitor cells.

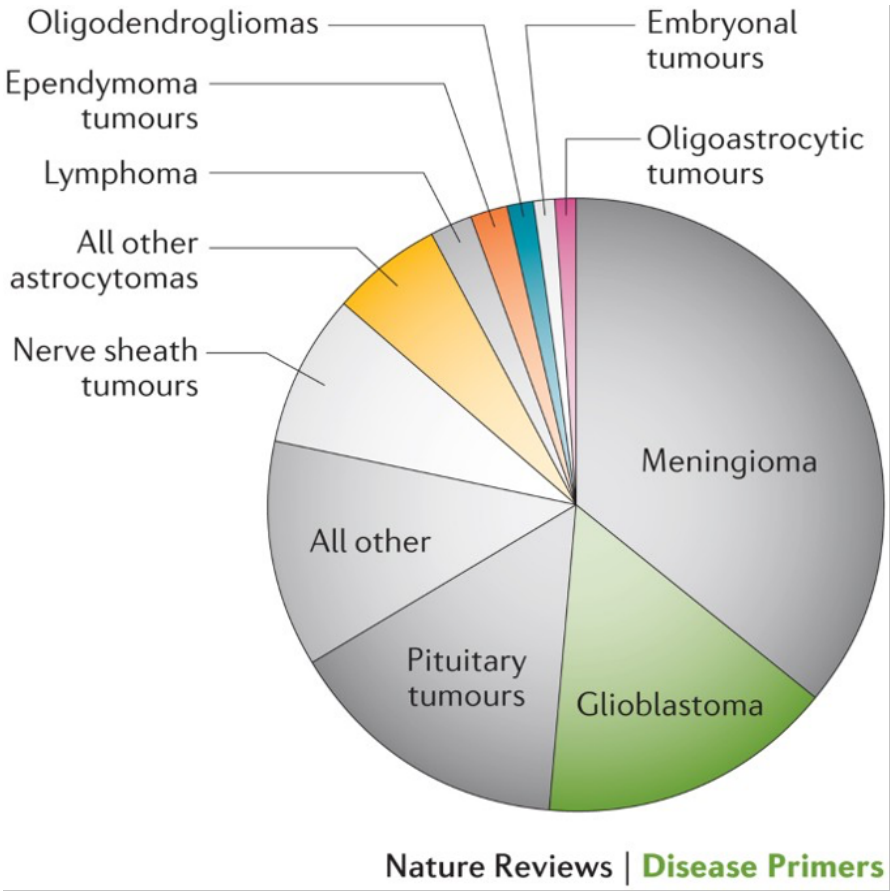

Figure 4. Patterns of distribution of primary tumors of the brain and central nervous system by relative frequency.

Health statistics show that primary brain tumors affected 21.4 patients per 100,000 during 2007 to 2011 in the United States and gliomas occurred in 6.6 persons per 100,000 while glioblastomas made up about half of this group [33]. The occurrence of pilocytic astrocytomas stood at 0.34 whereas diffuse astrocytomas displayed a count of 0.55 and oligodendroglial tumors recorded 0.36 and ependymomas noted 0.42 cases per 100,000 population (Fig. 5). Medical experts cannot determine the origin of low glioma occurrence in Japan since its numbers remain below half those in the United States and Northern Europe. The occurrence of gliomas rises as individuals grow older yet glioblastoma cases demonstrate the highest increase rate. Data shows that gliomas affect 0.15 children and 0.41 young people initially and eventually reach 13.1 individuals per 100,000 population in the 65-75 years age group until they reach 15.0 per 100,000 population in the age group of 75-84 years (Fig. 2). Research has not established the biological elements responsible for raising the likelihood of glioma growth among aging populations. The unexplained growth in

brain tumor prevalence remains unclear because population changes and more extensive diagnostic testing practices fail to account for the observation.

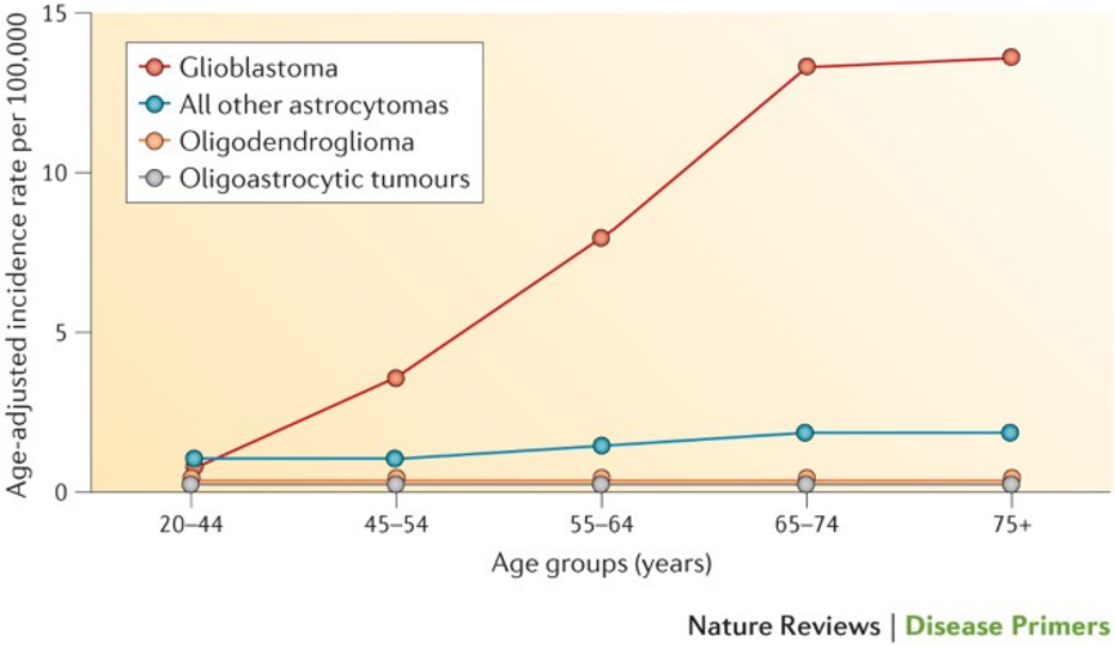

Figure 5. Age-related incidence rates of primary tumors of the brain and central nervous system (CNS), depending on the histology of the tumor and different age groups.

Gliomas are basically single-cell genetic disorders, just like the majority of other tumors. The clinical characteristics of brain tumors are shaped by certain patterns of genetic changes, which are also being utilized more and more for diagnostic and categorization reasons (Fig. 6).

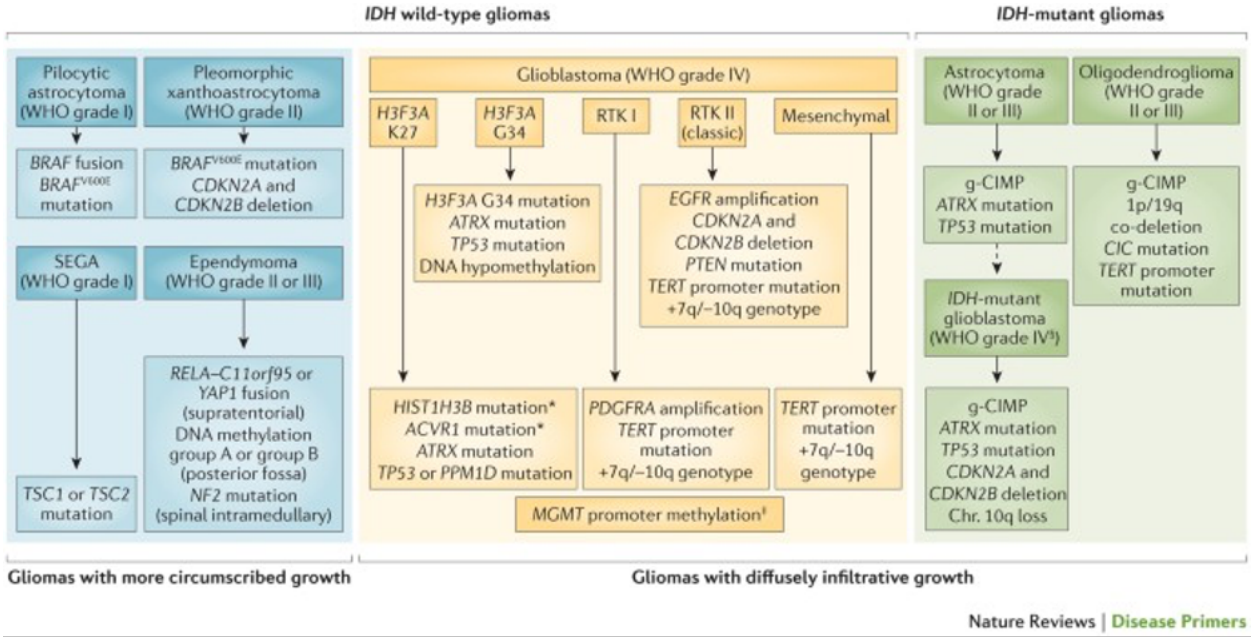

Figure 6. The figure shows the key genetic and epigenetic modifications usually associated with different types of gliomas, highlighting the molecular characteristics that distinguish them.

Three different brain tumors (pilocytic astrocytoma, pleomorphic xanthoastrocytoma, subependymal giant cell astrocytoma (SEGA)) comprise the majority of this group. These tumors occur in young children or adults and grow gradually while keeping a defined border. Patients diagnosed with neurofibromatosis type 1 (NF1) experience higher risk levels for pilocytic astrocytoma tumors because of probable NF1 gene mutations. Neurofibromin exists as a protein that comes from this gene. The protein functions as a key tumor suppressor to manage the mitogen-activated protein kinase (MAPK) signaling pathway [36]. Among the most significant identified genetic changes were shortened duplications and oncogenic fusions involving BRAF or RAF1 genes, both of which encode serine/threonine protein kinases. It was found that these changes, along with activating point mutations of BRAF V600E and mutations in the KRAS gene, sometimes affecting areas beyond the typical codons 12, 13 and 61, stimulate tumor development. In addition, recurrent genius mutations in the MARK signaling pathway, in addition to NF1 mutations, are usually observed in sporadic cases of pilocytic astrocytoma. It is important to note that new generation sequencing studies have shown that pilocytic astrocytoma is largely caused by changes within a single molecular pathway, while frequent mutations not detected outside this

pathway are not observed even in previously unexplained cases of tumors [37, 38,39,50]. There are several therapeutic implications and uses for the quickly developing knowledge of the molecular subtypes of gliomas (Table 1). Clinical trial design, pathologic testing needs, diagnostic imaging, and targeted glioma therapy are some of these uses.

Table 1. Emerging targeted therapies for glioma subtypes.

Subtype	Markers	Median age (years)	Emerging targeted therapies
Mesenchymal Glioblastoma	NF1 deletion NF-kappaB activation	58	Trametinib Eriotinib EGFR vaccines
Classical glioblastoma	EGFR amplification	52	Anti-EGFR antibody–drug conjugates
Midline gliomas	H3F3A K27M mutation	5–11	Glutaminase inhibitors Checkpoint nhibitors
ProneuraL/RTK glioblastomas	PDGFRA amplification $BRAFV_{600E}$ OD23 deletion	8	Dabrafenib Vemurafenib
Pilocytic astrocytoma	BRAF fusion	5–14	Sorafenib Immune checkpoint inhibitors
Giant cell glioblastoma	POLE mutation IDH mutation ATRX mutation	44	IDH inhibitors IDH vaccine
Diffuse astrocytoma	TP53 mutation IDH mutation	36	IDH inhibitors IDH vaccine
Diffuse oligoden droglioma	CIC or FUBP1 IDH vaicinioa	35–44	Imetelstat
Proglioblastoma	IDH wild type		Dabrafenib Vemurafenib
Pleomorphic xanthoastrocyctoma	$BRAF_{V600E}$ar mutation	22	Dabrafenib Vemurafenib
Gangliogliomas	$BRAF_{V600E}$ mutation	9–25	Dabrafenib Vemurafenib
Gangliogliomas	$BRAF_{V600E}$ mutation	9–25	

Through noninvasive imaging, the elevated levels of 2HG in IDH-mutated gliomas can be utilized as a biomarker. Numerous studies have demonstrated that magnetic resonance spectroscopy can identify high 2HG levels, and it may eventually be able to accurately determine if a tumor has an IDH mutation without requiring a biopsy [41, 42]. By determining the IDH mutation status of a suspected glioma before surgery, this innovative method may help neurosurgeons plan for the appropriate degree of resection. According to a recent retrospective analysis, the predictive connections of the extent of glioma resection of enhancing and non-enhancing sections differed significantly depending on the presence of an IDH mutation. Extensive resection of a non-increasing tumor volume significantly affected survival outcomes only in patients with gliomas with the IDH mutation. On the contrary, the volume of resection of the increasing tumor component was more closely associated with improved prognosis in cases of wild-type IDH gliomas [43].

Using machine learning systems, we identify patterns in vast datasets that make it impossible for humans to detect and generate predictions based on the data. Progressive technical collaborations between imaging research and computer science experts have elevated interest in using machine learning for medical image analysis particularly through radiomics analysis of primary brain tumors [44, 45]. The development of tumor genomic approaches and emerging personalized therapies will increase our benefits from machine learning technologies in brain tumor picture analysis despite high-grade glioma remaining a dangerous aggressive cancer. A rising number of scientific investigations implement machine learning alongside deep learning for brain tumor analysis during these recent years (Fig. 7).

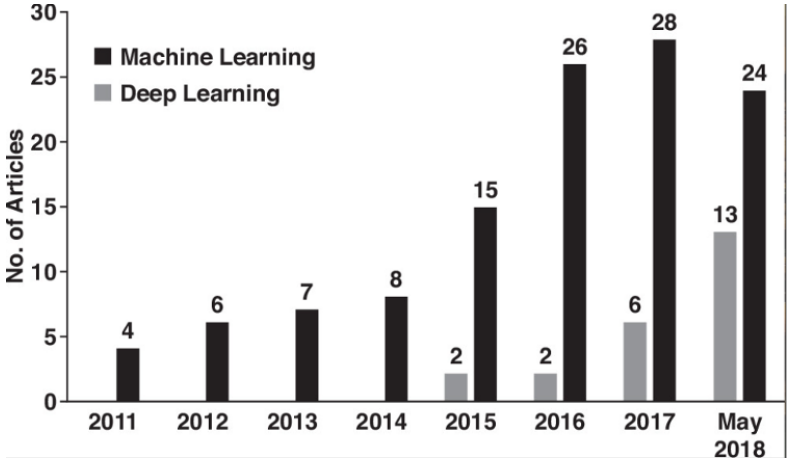

Figure 7. The graph illustrates the increasing trend in the number of publications found in PubMed each year, indicating a growing interest and research activity in the application of

machine learning and deep learning methods for the treatment of brain tumors and gliomas since 2011.

Glioma quantitative analysis must be simple, quick, and accurate in order to better inform clinical judgments about available treatments. Medical protocols for treatment primarily depend on bidirectional single-plane orthogonal measurements according to the criteria for assessing response in neuro-oncology (RANO) [46]. Large clinical trials and other major research projects depend on these coarse measurements of geometry. Three-dimensional volumetric assessment of the enlarging tumor and the surrounding peritumoral edema is expected to significantly improve treatment planning and assessment of tumor progression over time [47]. Because manual 3D segmentation techniques are laborious, subjective, and time-consuming, they have not become widely used [48]. Semiautomated and automatic glioma segmentation techniques are becoming more and more popular as a result of improvements in algorithm development and computer power (Fig. 8) [49].

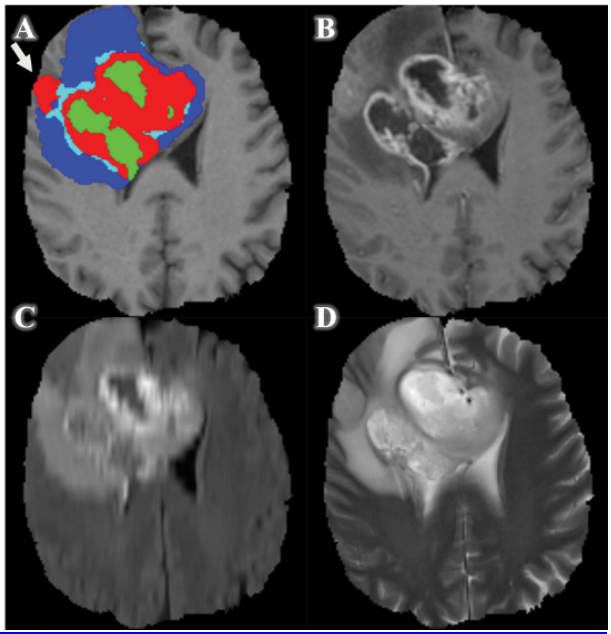

Figure 8. A 59-year-old male patient diagnosed with wild-type IDH glioblastoma was examined using semi-automatic brain tumor segmentation techniques. (A) The fused segmented image illustrates the various components of the tumor, including the enlarging area (red), the necrotic nucleus (green), the non-enlarging tumor (light blue), and the surrounding edema (dark blue). The segmentation software successfully identified and outlined the enlarging area (indicated by

the arrow) separately from the main enlarging tumor nucleus; However, such segmentation processes remain time-consuming and require significant manual effort. (B) In addition, MRI images with T1-weighing, (C) FLAIR, and (D) T2-weighing with increased contrast, processed by cranial autopsy methods using commercially available software, are presented.

Work in this field has shifted to machine learning techniques throughout the last ten years. Brain tumor segmentation can be viewed as a voxel-level classification challenge from a machine learning standpoint, determining whether a particular voxel is part of the glioma, edema, or normal brain classes. These techniques fall into two major categories: deep learning with convolutional neural networks (CNNs), which has dominated the field in recent years and outperformed classic machine learning techniques [50, 51, 52] and hand-engineered features and classifier methods based on classic machine learning, such as support vector machines (SVM) and random forests [53, 54].

2.2.3. Meningioma

Meningioma makes for 37.6% of all malignancies of the central nervous system and is the most prevalent primary intracranial tumor [55]. About 20% of all meningiomas are high-grade (WHO grade II–III) meningiomas, which are linked to a worse prognosis and a greater recurrence rate. The prognosis for meningiomas is not always good, even though the majority of them are benign (WHO Grade I). One histological indicator that is often associated with tumor progression is the Ki-67 index, whose high expression usually denotes unchecked and rapid cell proliferation [4]. According to mounting data, a high Ki-67 index is a direct predictor of prognosis and is linked to a higher likelihood of recurrence after surgical resection. Predicting meningioma patients' grade noninvasively and reducing the amount of time they need to be monitored before surgery are crucial [56, 57, 58].

Two experienced radiologists, each with more than five years of experience in image interpretation, carefully analyzed eight key radiological characteristics. These signs included peritumoral edema, the presence of cerebrospinal fluid (CSF) around the tumor, capsule enlargement, heterogeneous structures of enlargement, intracellular necrosis, spread to the phallus or tentorium, the presence of a dura mater tail, and signs of invasion of surrounding tissues. To

find clinical and radiological characteristics that were substantially connected with various grades, Ki-67, and their combination groups, univariate and multivariate analyses were conducted. For clinical and radiological characteristics, both univariate and multivariate analyses were deemed statistically significant if the P value was less than 0.05. To construct the CRR model, features that demonstrated statistical significance in both univariate and multivariate studies were chosen. Two case examples are displayed in Figure 9 [59].

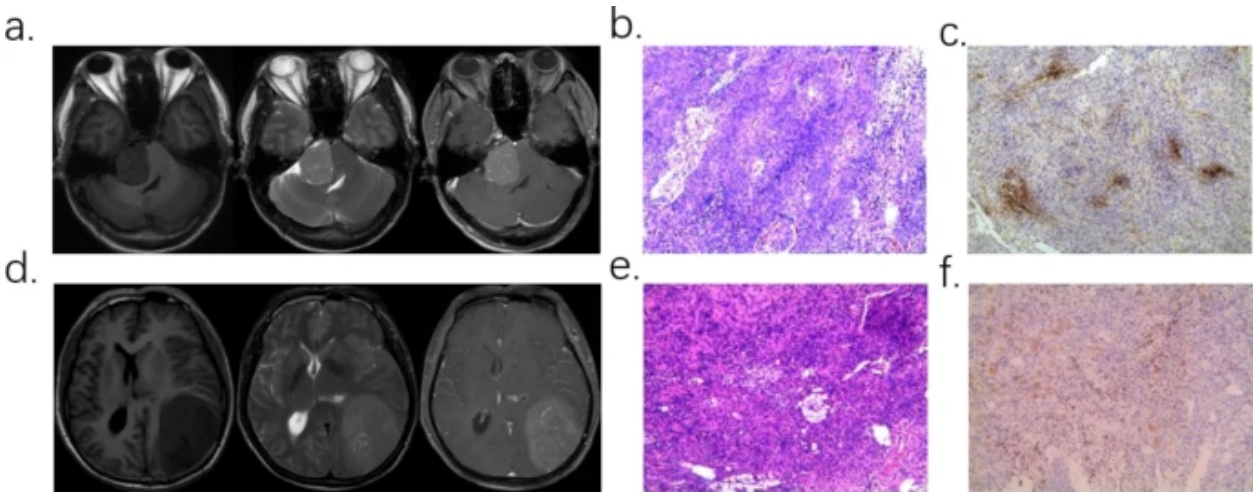

Figure 9. Two illustrative examples are presented. (a–b) In a patient diagnosed with grade I meningioma according to the WHO classification, the Ki-67 proliferation index is 5-10%. (a) MRI images include T1-weighted, T2-weighted, and contrast-enhanced T1 sequences. (b–c) The corresponding pathological sections and the results of immunohistochemical staining are shown. (d–f) In another case, we were talking about a patient with grade II meningioma according to the WHO classification, whose Ki-67 index was 2-3%. (d) the MRI sequences (T1WI, T2WI and T1CE) are displayed, as well as (e–f) the corresponding histopathological and immunohistochemical data.

AutoRadiomics, created by Woznicki et al., is the source of the radiomics machine learning pipeline utilized in this investigation (Fig. 10). In addition to their work, bootstrapping methods, deep learning feature extraction, and other optimizations were applied [60].

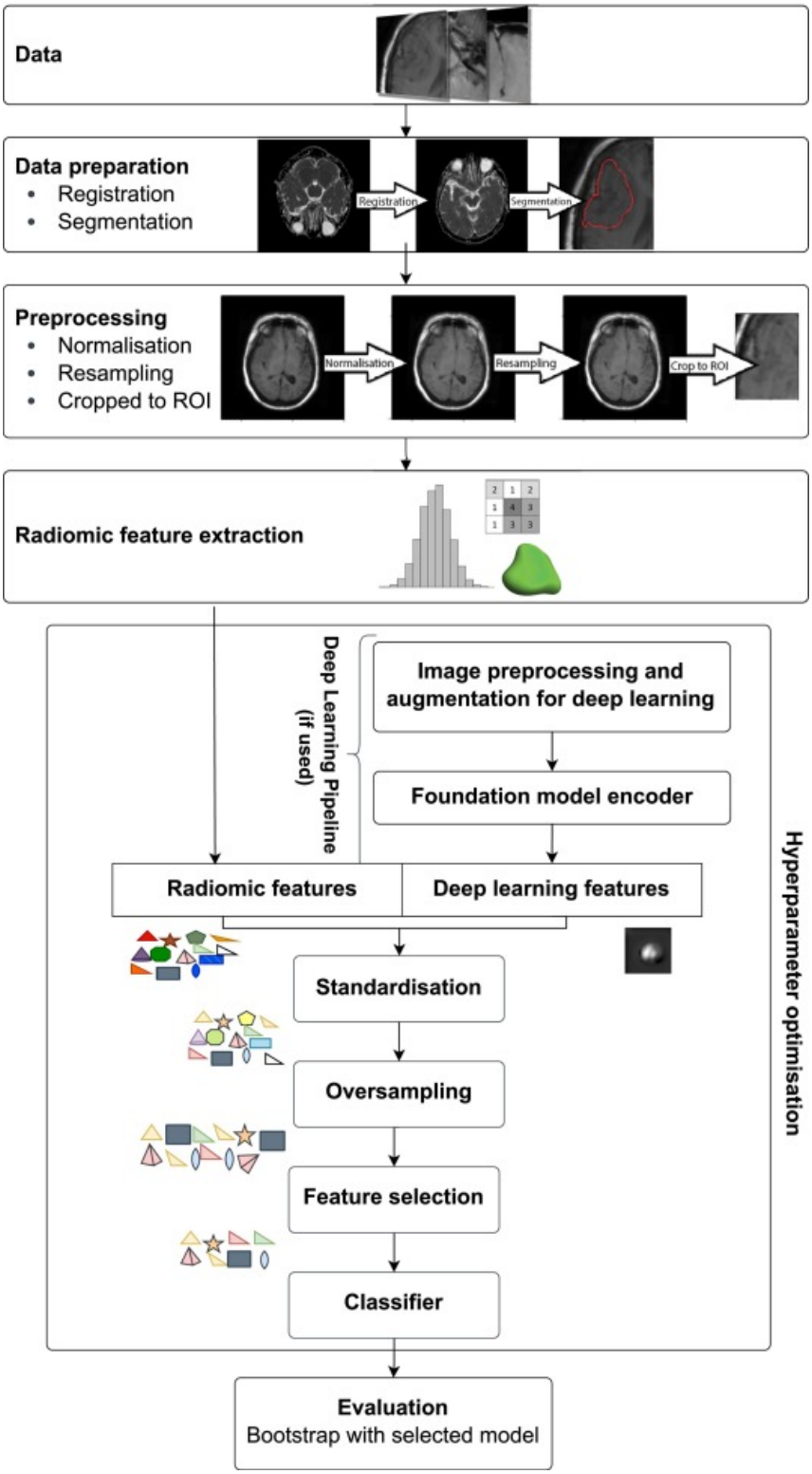

Figure 10. An overview of the workflow in the field of radiomics and machine learning, illustrating the key steps, starting with data collection and then data preparation, image preprocessing, feature extraction and model development. In addition, the pipeline may include

feature extraction methods based on deep learning. The return on investment relates to the region of interest.

PyRadiomics version 3.1.0, which included picture preprocessing before extraction, was used to extract handcrafted radiomics [61]. This required scaling with a factor of 500 after standardizing to a mean of 0 and a standard deviation of 1. After cropping the images to the ROI, they were resampled using linear interpolation to achieve consistent pixel spacing [62]. Histogram-based features were calculated using a voxel array shift of 1000 and a bin width of 25, which were empirically determined to guarantee firstorder_ For all photos, the range split by bin width falls between 16 and 128 bins. With feature_extraction_config.yaml supplied in Supplementary Data S1, all other parameters in PyRadiomics stayed at their default settings. The distinctions between PyRadiomics and the Image Biomarker Standardization Initiative are described in Supplementary Data S2. We ended each feature name with the name of the imaging modality. A total of 5185 handmade radiomic features were produced by utilizing all accessible features, with 1037 characteristics per picture modality. The extracted objects included 19 first-order statistical objects, 14 shape-related objects, and various textural objects obtained from several matrices, such as the gray-level match matrix (GLCM, n = 24), the gray-level run length matrix (GLRLM, n = 16), and the zone size matrix. at the gray level (GLSZM, n = 16), the gray level dependence matrix (GLDM, n = 14) and the neighboring gray difference matrix (NGTDM, n = 5). In addition, three types of image filters were applied — initial, wavelet, and Gaussian Laplace (LoG) — using sigma values of 3.0 and 5.0 to further improve feature extraction [63].

2.3. Suggested Approach

In this study, axial slices of MRI images were used as input data for the classification process. These MRI slices were introduced into a neural network model that was responsible for both feature extraction and classification tasks, as shown in Figure 11 [64]. In essence, the classifier is a CNN model that assigns the image to one of two categories: Demented or NonDemented. For the classifier CNN block, a pre-trained ResNet-101 model has been utilized.

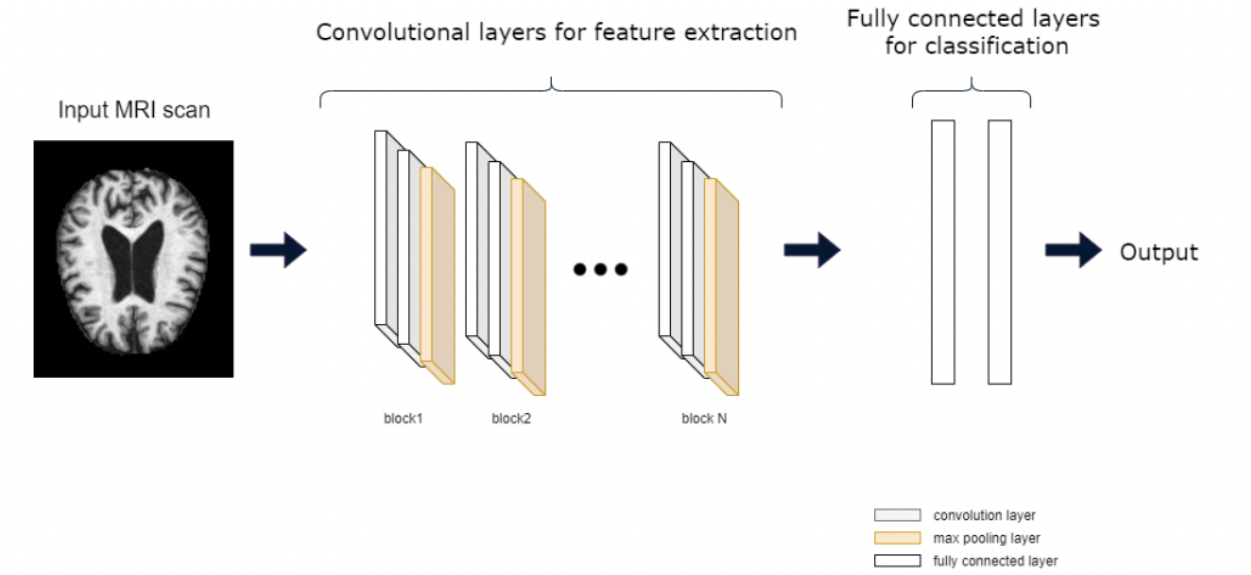

Figure 11. The suggested technique for classifying Alzheimer's disease from slices of brain MRI images is shown in a block diagram [64]

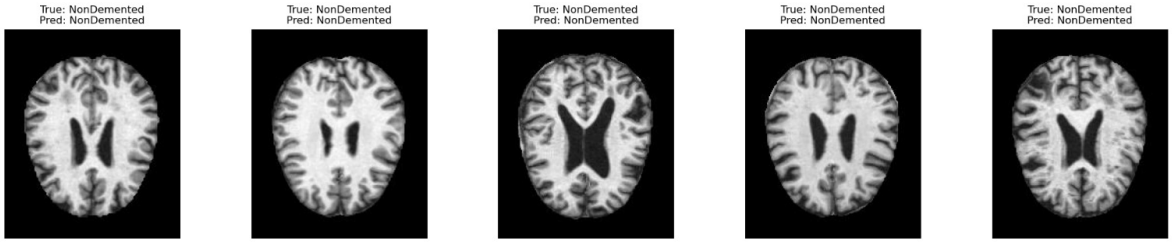

Figure 12. MRI imaging of a healthy-nondemented brain: basic structural features used for comparison and training in deep learning models for detecting Alzheimer's disease.

A series of MRI images of the brain belonging to the "Healthy" class, as well as the corresponding predictions of the model (Fig. 12). In all five cases shown, the model successfully identified the images as "Healthy", demonstrating its ability to correctly classify healthy brain structures.

The images demonstrate typical characteristics of a healthy brain, such as well-defined cortical boundaries, normal ventricular size, and the absence of abnormal structural changes or lesions. These features were effectively studied by the deep learning model during training, which allowed it to distinguish images of people who do not suffer from insanity from images affected by Alzheimer's disease or other neurological disorders.

The correct predictions in these examples highlight the model's power in recognizing the structural features of a healthy brain and minimizing false positives in classification tasks using MRI.

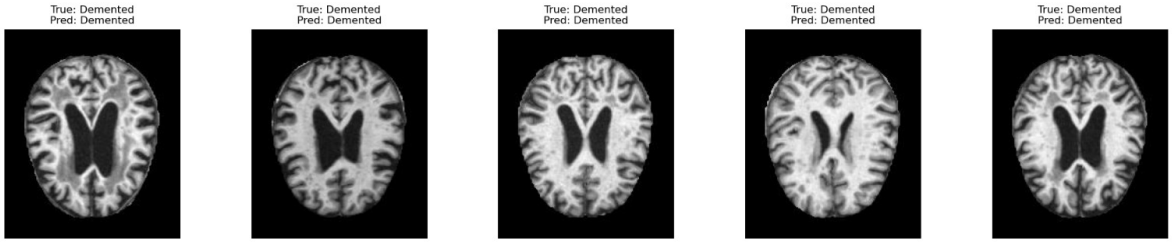

Figure 13. MRI-based visualization of Alzheimer's disease progression: Brain structural changes used to detect deep learning and classify the stages of dementia.

A collection of MRI brain scans from the dementia class (Alzheimer's disease), as well as model predictions that correlate with the images (Fig. 13). The algorithm was able to identify anatomical brain changes often associated with Alzheimer's disease, accurately classifying the photos as related to dementia in each of the five presented examples. These MRI scans show typical symptoms of dementia, including ventricular enlargement, critical thinking, and marked brain atrophy. The cause of these changes is the progressive loss of brain tissue, which is the main sign of Alzheimer's disease. The model successfully identified these minor but important visual changes in the MRI images.

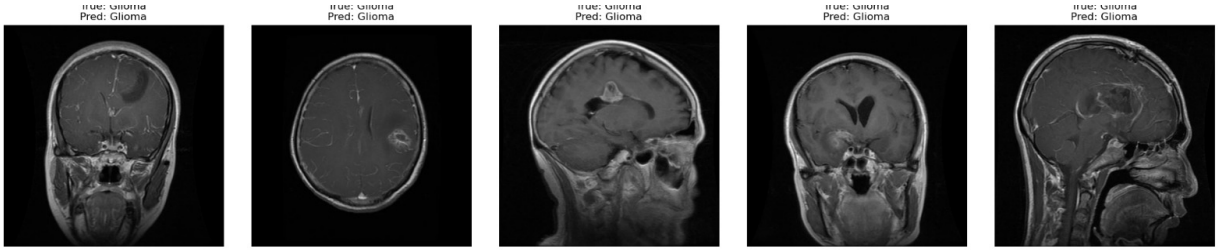

Figure 14. MRI imaging of glioma tumors: Structural abnormalities for the detection, segmentation, and classification of brain tumors based on deep learning.

A set of MRI images of the brain from the glioma class, demonstrating examples when the deep learning model correctly classified the images (Fig. 14). In all five cases, the true signs

and predictions of the model coincided with glioma, which indicates the high accuracy of the model in detecting this type of brain tumor. Glioma tumors are typically characterized by irregular shapes, varying intensity, and visible mass effects in the brain structure, all of which are visible in the displayed images. The model was able to successfully recognize these features on different MRI slices and in different orientations (axial, sagittal, and coronary views).

These results confirm the effectiveness of the model in studying glioma-specific patterns and its ability to accurately distinguish glioma from other brain diseases, minimizing false negative results and ensuring reliability in tumor detection tasks.

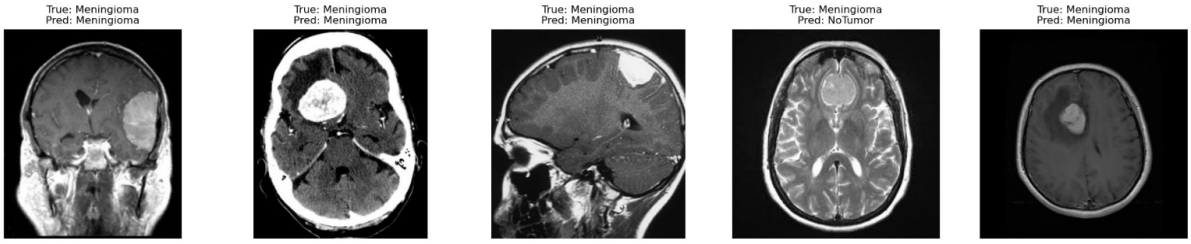

Figure 15. Visualization of MRI images for a class of meningiomas with model predictions.

Figure 15 shows a set of brain MRI images from a test dataset illustrating examples from the meningioma class, as well as the corresponding predictions generated using the proposed model. The first, second, third and fifth images were successfully identified by the model as a meningioma, which indicates its ability to recognize typical signs of a tumor, such as irregular borders, differences in intensity and specific localization of the tumor in the brain structure. However, the fourth image demonstrates a case of misclassification, when the model incorrectly identified a meningioma tumor as non-cancerous. This error can be explained by the low contrast or fuzzy boundaries of the tumor area, which makes it visually resemble healthy brain tissue and thus contributes to incorrect prediction of the model.

Figure 16. Visualization of MRI images for a tumor-free classroom with model predictions.

A series of MRI scans of the brain from the "Tumor-free" class, demonstrating cases where the proposed deep learning model correctly determined the absence of tumors (Fig. 16). In all five examples presented, the main sign of the model's truth and prediction coincide - there are no tumors, which indicates the high reliability and accuracy of the model in recognizing healthy brain structures. MRI scan demonstrates the normal anatomy of the brain without any noticeable structural abnormalities or formations. The model successfully recognized these features, confirming its ability to distinguish healthy brain tissue from pathological changes usually associated with brain tumors or neurological disorders.

These results highlight the effectiveness of the model in detecting malignant brain tumors and minimizing false positive predictions, which is important to ensure reliability in clinical settings.

2.4. Accessible Datasets

Brain tissue types (CSF, GM, and WM) and AD patients are classified using the data evaluation framework of three-dimension (3D) cross-sectional brain MRI. In this sresearch, a total of 9,607 MRI images were utilized for model training and evaluation (Table 2). The dataset included four distinct classes: Demented (2560 images), Glioma (1321 images), Meningioma (1571 images) and Non-Demented (Healthy) (2560 images), and No Tumor (1595 images). These MRI scans were essential for developing and validating the deep learning-based classification model aimed at detecting and differentiating between Alzheimer’s disease, brain tumors, and healthy brain conditions.

Table 2. Distribution of MRI Pictures of the Brain Used to Train and Assess Models.

Class	Number of Images	Description
Demented	2560	MRI scans of patients diagnosed with Alzheimer’s disease
Glioma	1321	MRI scans showing glioma-type

		brain tumors
Meningioma	1571	MRI scans containing meningioma-type tumors
Non-Demented (Healthy)	2560	MRI scans of healthy individuals (control group)
No Tumor	1595	Tumor-free MRI scans, including non-demented brains from the Br35H dataset
Total	9607	

2.4.1. Dataset for Alzheimer's Disease

Google Colab is used to conduct the experiment. During the training, a hardware accelerator on the GPU is used. The Kaggle AD dataset contains 1,279 test samples for testing and 5,121 training data samples. The samples were divided into four categories: Dementia There are three types of dementia: very mild, moderate and moderate [64].

As part of a Kaggle competition, 6400 magnetic resonance images were gathered and made public. Depending on the degree of neurological degeneration, MR images are classified as non-demented, very slightly demented, mildly demented, and moderately demented. Nonetheless, three components of the demented group were broadly categorized as demented in this analysis. A non-overlapping train set and a test set are created from the entire dataset. There are 1279 photos in the test set and 5121 images in the training set. Certain classes, such as those with moderate dementia, are underrepresented. During training, data augmentation is employed to equalize the class variability [65].

2.4.2. Dataset for Brain Tumor

Figshare, SARTAJ, and Br35H are three publically available datasets that were combined to create the dataset utilized in this study for training and assessing the deep learning model. The 7,023 brain MRI scans in the integrated dataset are divided into four different classes: pituitary tumor, meningioma, glioma, and no tumor (healthy brain) [66].

The Br35H dataset, which offers a complete collection of normal brain MRI scans, is noteworthy for having the only images that correspond to the no tumor class [66]. These datasets were combined to guarantee a balanced and varied depiction of brain states, which improved the suggested deep learning model's resilience for tasks involving the detection and classification of brain tumors.

Chapter 3 – (RESULTS AND DISCUSSION)

3.1. Overall Model Performance

Once the model was trained, its performance was tested on unseen data. The results showed that the model performed quite well, achieving a test accuracy of 89.52%.

Table 3. The detailed performance metrics.

Test accuracy	Test Loss	Precision	Recall	F1-Score
89.52%	0.4581	92.28%	92.16%	92.17%

These outcomes indicate that the model was capable of correctly classifying most images and adapting well to new data, particularly for tumor detection tasks.

3.1.1. Class-Wise Performance

Table 4. Detailed breakdown of the model's performance for each class.

Class	Precision	Recall	F1-Score	Support
Demented	0.85	0.78	0.81	639
Glioma	0.99	0.99	0.99	300
Meningioma	0.99	0.98	0.99	306
Non-Demented	0.80	0.86	0.83	639
No Tumor	0.99	1.00	0.99	405

The model showed excellent accuracy for tumor classes, while performance for Alzheimer's disease detection was slightly lower, which is expected due to the subtle nature of changes in dementia patients' MRI scans.

3.1.2. Confusion Matrix Analysis

Figure 17 shows the confusion matrix generated during testing. This matrix visualizes how well the model was able to correctly classify each class, while also highlighting the main errors.

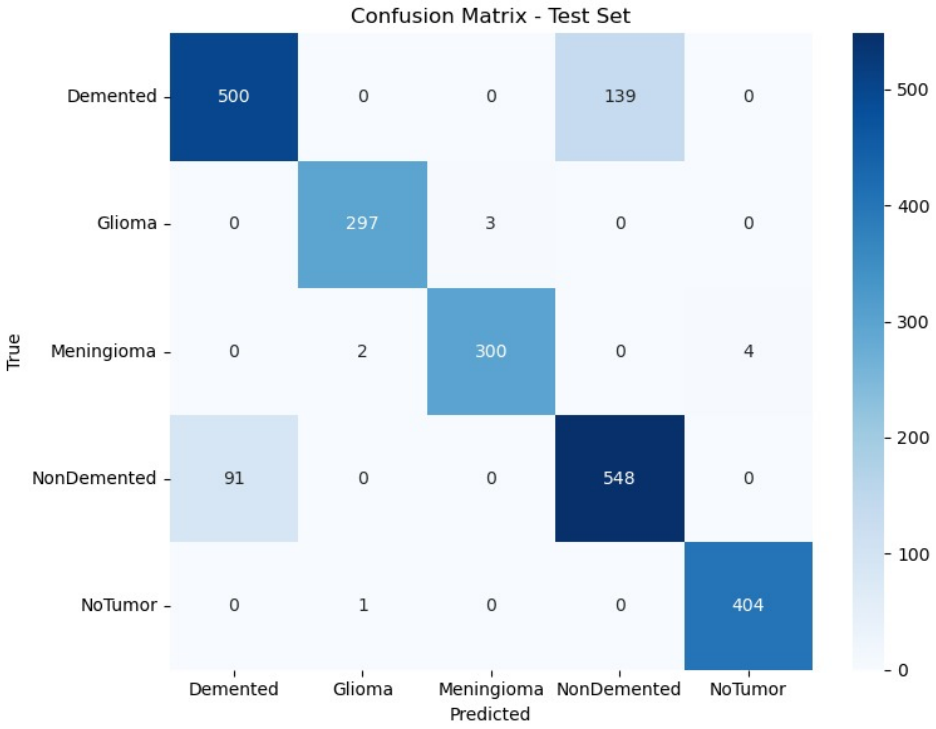

Figure 17. The proposed deep learning model's confusion matrix on the test dataset.

Key findings include:

- Non-Demented: 548 correct predictions
- Demented: 500 correct predictions
- No Tumor: 404 correct predictions
- Meningioma: 300 correct predictions
- Glioma: 297 correct predictions

The majority of errors were found between Demented and Non-Demented classes:

- 139 Demented images misclassified as Non-Demented
- 91 Non-Demented images misclassified as Demented

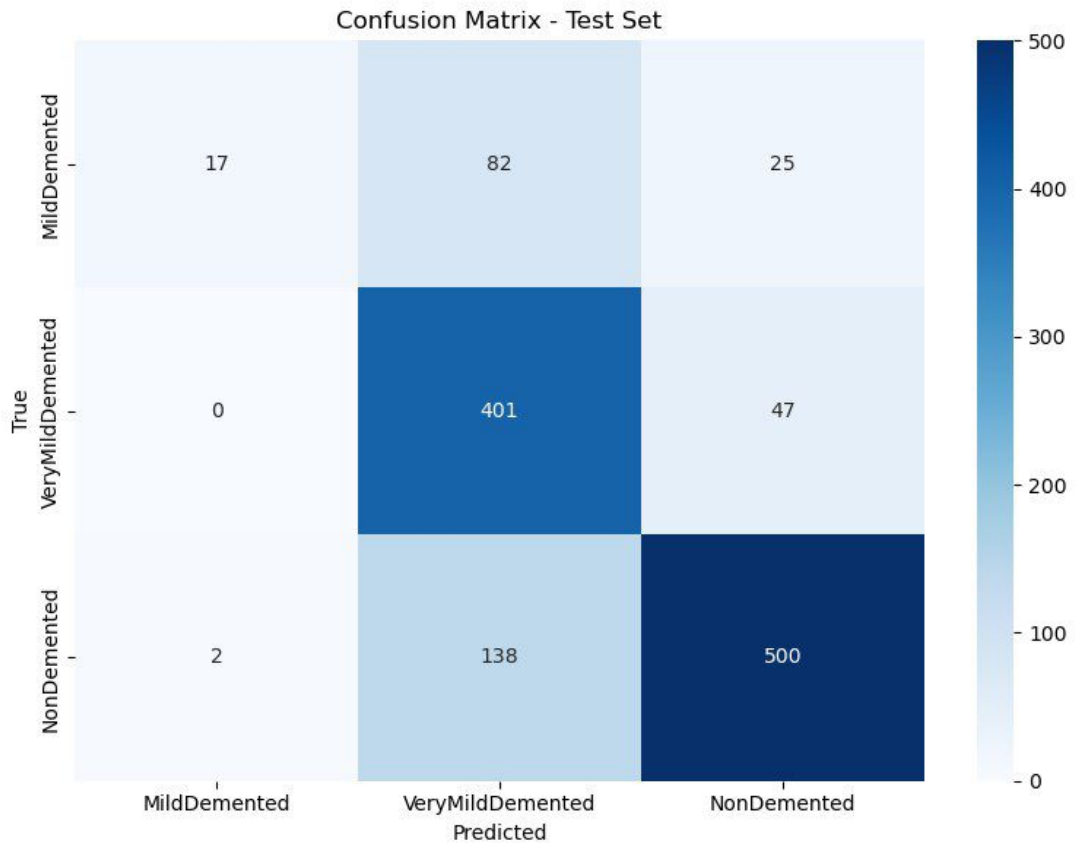

Figure 18. Confusion Matrix for the Test Set in Alzheimer's Disease Classification

This visualization explains how well the deep learning model performed on the testing dataset on classifying Alzheimer's disease into three groups, namely: Mild Demented, Very Mild Demented, and Non-Demented classes (Fig. 18). The diagonal figures tell how many instances were correctly predicted in each class. Off-diagonal values show misclassifications, i.e., places where the model wrongly classified a sample to a different class.

The model's correct classification of 401 cases as Very Mild Demented indicated it is effective when detecting early stage dementia. On the other hand, a significant number of Non-Demented patients (138) were mislabeled as Very Mild Demented, which may reflect some

overfitting or uneven distribution of classes. Detection for Mild Demented cases was not as exact, 17 cases were correctly classified, but 82 of the cases were mislabeled as Very Mild Demented.

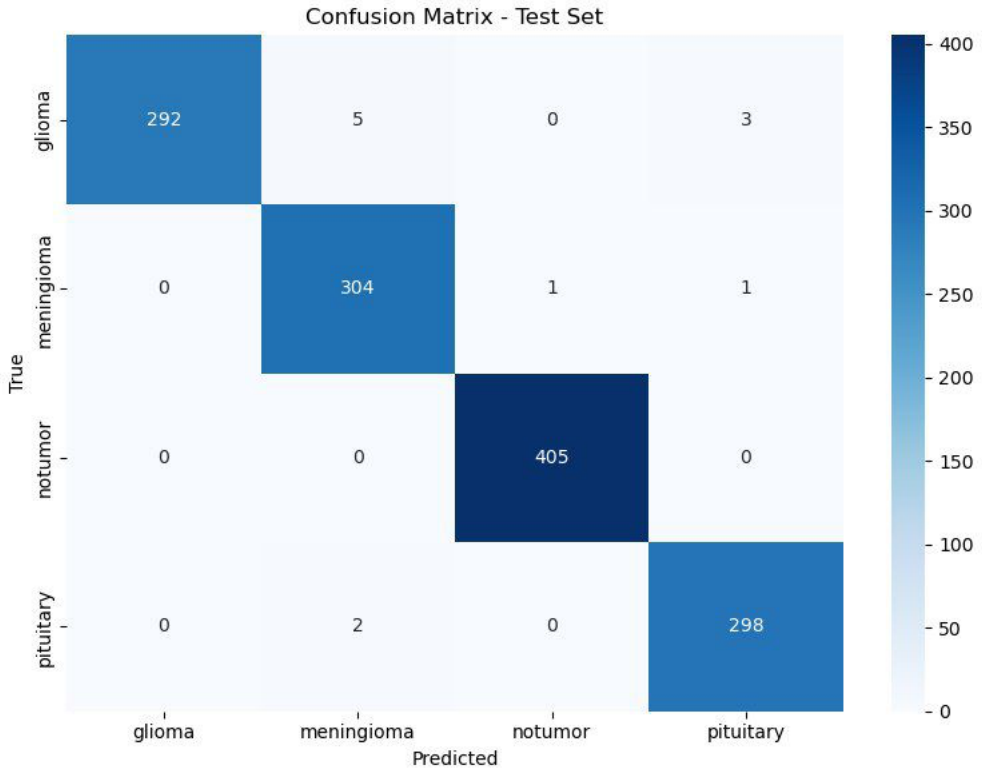

Figure 19. Confusion Matrix for Brain Tumor Classification on Test Set

Here, we examine a deep learning model's ability to classify brain MRI images into the four mutually exclusive classes:

- Glioma
- Meningioma
- No Tumor
- Pituitary Tumor

The model reports excellent accuracy in all four categories with an ideal classification for the No Tumor category (Fig. 19). The model provides some misclassification on a few glioma and pituitary, MRI imaging could explain some of these overlaps. Meningiomas and pituitary tumors

were the classes the model most frequently confused, probably due to vague borders of the tumors or overlapping patterns of intensity on MRI scans.

3.2. Visual Interpretation of Model Accuracy

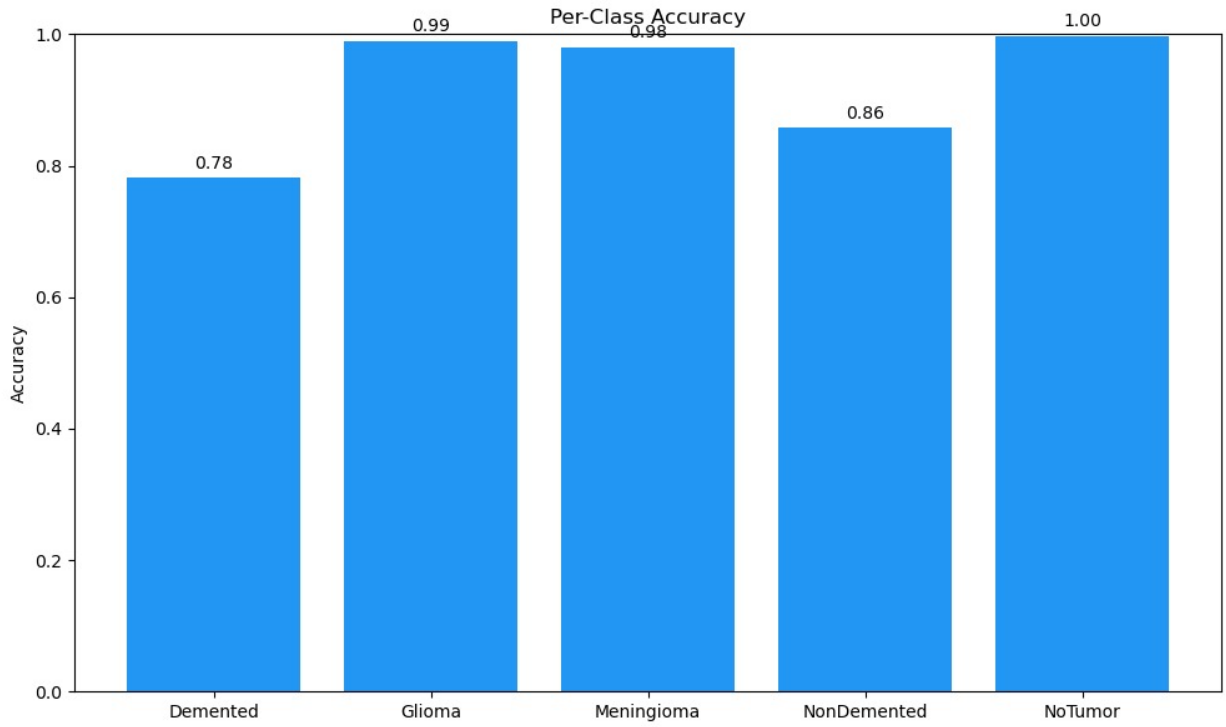

Figure 20. Per-Class Accuracy of the Proposed Deep Learning Model.

The per-class accuracy chart shows the highest performance in detecting Glioma (99%), Meningioma (98%), and No Tumor (100%). Non-Demented images were classified with an accuracy of 86%, while Demented images showed the lowest accuracy at 78% (Fig. 20).

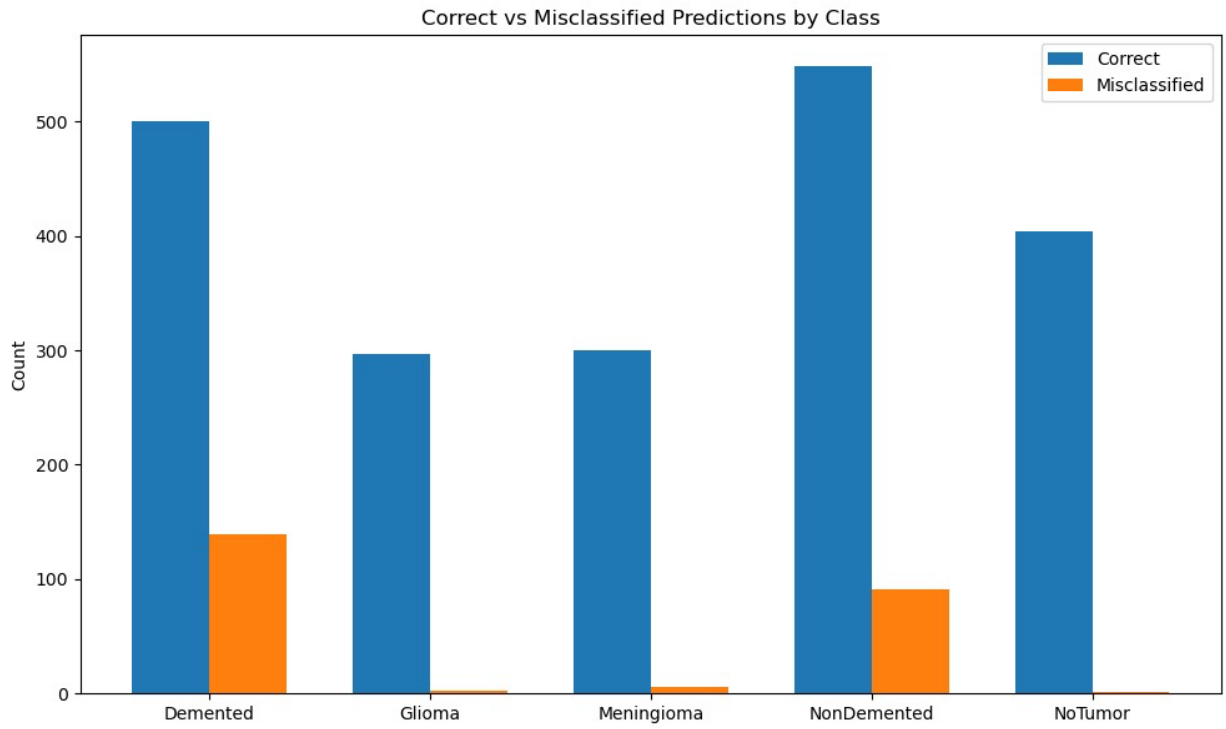

Fig 21. Distribution of Correct vs Misclassified Predictions for Each Class.

Figure 21 demonstrates the number of correct and incorrect predictions per class. The majority of misclassifications happened in distinguishing Demented from Non-Demented images, which reflects the challenge of identifying early-stage Alzheimer's disease through MRI scans.

3.3. Observed Limitations

Although the model demonstrated strong overall performance, several limitations were observed during the study:

- Difficulty in differentiating Alzheimer’s disease from healthy brains due to subtle visual differences.
- Class imbalance, particularly between tumor and non-tumor images.
- Variability in image quality and acquisition settings from multiple open-source datasets.
- Absence of clinical information such as age, gender, and medical history, which could have enhanced model interpretation.

3.4. Summary of Key Findings

The proposed deep learning model showed promising results in classifying brain MRI images across five distinct categories. It achieved outstanding accuracy for tumor detection and reasonable accuracy for Alzheimer's disease classification. The results demonstrate the potential of using deep learning techniques to support radiologists in the early diagnosis of neurological disorders, although further improvement is necessary for dementia-related classifications.

CHAPTER 4 - (CONCLUSION)

Conclusion

A deep learning-based classification model for the early detection and differentiation of neurological diseases was effectively created and evaluated using MRI brain scans. The main objectives of the study were to classify healthy brain conditions and identify malignant brain tumors, including gliomas and meningiomas, as well as Alzheimer's disease.

To train the model, 9607 MRI scans were used, which were divided into five classes: Dementia (Alzheimer's disease), glioma, meningioma, incapacitated (healthy) and without tumors. Without the need to develop human characteristics, the model was able to automatically extract and study key characteristics from MRI scan results using convolutional neural networks (CNNs).

The experimental results showed that the proposed model performed well in classification with an overall accuracy of 89.52%. When it came to identifying brain tumors, in particular gliomas, meningiomas, and non-tumor conditions, the model demonstrated exceptional accuracy and responsiveness. However, due to the fact that dementia at an early stage and healthy brain structures differ slightly, it was more difficult to classify Alzheimer's disease. According to the Confusion Matrix study, mentally retarded and incapacitated people were most often misclassified.

Despite these obstacles, the proposed model has demonstrated encouraging potential for use as an additional tool in medical diagnostics. It can help practitioners make clinical decisions by automatically and efficiently classifying various neurological diseases based on MRI scan results, allowing for earlier intervention and therapy planning.

However, the study also has some drawbacks, such as an imbalance of dataset classes, differences in image quality, and a lack of clinical data on specific patients such as age, gender, or disease stage. By using multimodal imaging data, including larger and more balanced datasets, and exploring advanced deep learning approaches to better classify neurodegenerative diseases, future research may aim to overcome these limitations.

With all of the above in mind, this study advances the expanding field of artificial intelligence applications in medical imaging and shows how deep learning can help in the early detection of neurological diseases.

REFERENCE LIST

[18] Akkus, Z., Galimzianova, A., Hoogi, A., Rubin, D. L., & Erickson, B. J. (2017). Deep Learning for Brain MRI Segmentation: State of the Art and Future Directions. Journal of Digital Imaging, 30(4), 449–459. https://doi.org/10.1007/s10278-017-9983-4

[62] Albahrani, F. H., Alturaiki, J. A., Alahmed, A. Y., Aljasem, J. M., Alshammari, M. M., Alali, A. S., Aldabbab, A. Y., Alhelal, A. A., & Alkhairy, A. (2024). Co-occurrence of meningioma and intracranial aneurysm: a systematic review. Cureus. https://doi.org/10.7759/cureus.52919

[65] alzheimers-dataset-4-class-of-images. (2023, April 12). Kaggle. https://www.kaggle.com/datasets/preetpalsingh25/alzheimers-dataset-4-class-of-images

[23] Alzheimer's Disease facts and figures. (n.d.). Alzheimer's Association. https://www.alz.org/alzheimers-dementia/facts-figures#:~:text=,are%20age%2075%20or%20older

[25] Barker, W. W., Luis, C. A., Kashuba, A., Luis, M., Harwood, D. G., Loewenstein, D., Waters, C., Jimison, P., Shepherd, E., Sevush, S., Graff-Radford, N., Newland, D., Todd, M., Miller, B., Gold, M., Heilman, K., Doty, L., Goodman, I., Robinson, B., . . . Duara, R. (2002). Relative frequencies of Alzheimer disease, lewy body, vascular and frontotemporal dementia, and hippocampal sclerosis in the state of Florida Brain Bank. Alzheimer Disease & Associated Disorders, 16(4), 203–212. https://doi.org/10.1097/00002093-200210000-00001

[43] Beiko, J., Suki, D., Hess, K. R., Fox, B. D., Cheung, V., Cabral, M., Shonka, N., Gilbert, M. R., Sawaya, R., Prabhu, S. S., Weinberg, J., Lang, F. F., Aldape, K. D., Sulman, E. P., Rao, G., McCutcheon, I. E., & Cahill, D. P. (2013). IDH1 mutant malignant astrocytomas are more amenable to surgical resection and have a survival benefit associated with maximal surgical resection. Neuro-Oncology, 16(1), 81–91. https://doi.org/10.1093/neuonc/not159

[66] Brain Tumor MRI dataset. (2021, September 24). Kaggle. https://www.kaggle.com/datasets/masoudnickparvar/brain-tumor-mri-dataset

[50] Brain tumor segmentation using convolutional neural networks in MRI images. (2016, May 1). IEEE Journals & Magazine | IEEE Xplore. https://ieeexplore.ieee.org/abstract/document/7426413/

[41] Choi, C., Ganji, S. K., DeBerardinis, R. J., Hatanpaa, K. J., Rakheja, D., Kovacs, Z., Yang, X., Mashimo, T., Raisanen, J. M., Marin-Valencia, I., Pascual, J. M., Madden, C. J., Mickey, B. E., Malloy, C. R., Bachoo, R. M., & Maher, E. A. (2012). 2-hydroxyglutarate detection by magnetic resonance spectroscopy in IDH-mutated patients with gliomas. Nature Medicine, 18(4), 624–629. https://doi.org/10.1038/nm.2682

[30] DeTure, M. A., & Dickson, D. W. (2019). The neuropathological diagnosis of Alzheimer's disease. Molecular Neurodegeneration, 14(1). https://doi.org/10.1186/s13024-019-0333-5

[52] Dvořák, P., & Menze, B. (2016). Local Structure Prediction with Convolutional Neural Networks for Multimodal Brain Tumor Segmentation. In Lecture notes in computer science (pp. 59–71). https://doi.org/10.1007/978-3-319-42016-5_6

[44] Erickson, B. J., Korfiatis, P., Akkus, Z., & Kline, T. L. (2017). Machine learning for medical imaging. Radiographics, 37(2), 505–515. https://doi.org/10.1148/rg.2017160130

[32] Ferlay, J., Parkin, D., & Steliarova-Foucher, E. (2010). Estimates of cancer incidence and mortality in Europe in 2008. European Journal of Cancer, 46(4), 765–781. https://doi.org/10.1016/j.ejca.2009.12.014

[31] Gavrilovic, I. T., & Posner, J. B. (2005). Brain metastases: epidemiology and pathophysiology. Journal of Neuro-Oncology, 75(1), 5–14. https://doi.org/10.1007/s11060-004-8093-6

[9] Ghosh, S., Das, N., Das, I., & Maulik, U. (2019). Understanding Deep Learning Techniques for Image Segmentation. ACM Computing Surveys, 52(4), 1–35. https://doi.org/10.1145/3329784

[45] Giger, M. L. (2018). Machine learning in medical imaging. Journal of the American College of Radiology, 15(3), 512–520. https://doi.org/10.1016/j.jacr.2017.12.028

[56] Goldbrunner, R., Stavrinou, P., Jenkinson, M. D., Sahm, F., Mawrin, C., Weber, D. C., Preusser, M., Minniti, G., Lund-Johansen, M., Lefranc, F., Houdart, E., Sallabanda, K., Rhun, E. L., Nieuwenhuizen, D., Tabatabai, G., Soffietti, R., & Weller, M. (2021). EANO guideline on the diagnosis and management of meningiomas. Neuro-Oncology, 23(11), 1821–1834. https://doi.org/10.1093/neuonc/noab150

[48] Gordillo, N., Montseny, E., & Sobrevilla, P. (2013). State of the art survey on MRI brain tumor segmentation. Magnetic Resonance Imaging, 31(8), 1426–1438. https://doi.org/10.1016/j.mri.2013.05.002

[40] Gronych, J., Korshunov, A., Bageritz, J., Milde, T., Jugold, M., Hambardzumyan, D., Remke, M., Hartmann, C., Witt, H., Jones, D. T., Witt, O., Heiland, S., Bendszus, M., Holland, E. C., Pfister, S., & Lichter, P. (2011). An activated mutant BRAF kinase domain is sufficient to induce pilocytic astrocytoma in mice. Journal of Clinical Investigation, 121(4), 1344–1348. https://doi.org/10.1172/jci44656

[17] Hsiao, C.-J., Hing, E., & Ashman, J. (2014). Trends in electronic health record system use among office-based physicians: United States, 2007-2012. National Health Statistics Reports, 75, 1–18. https://pubmed.ncbi.nlm.nih.gov/24844589/

[1] Islam, J., Zhang, Y. (2018). Brain MRI analysis for Alzheimer's disease diagnosis using an ensemble system of deep convolutional neural networks. Brain Inf., 5(2). https://doi.org/10.1186/s40708-018-0080-3

[22] Jack, C. R., Knopman, D. S., Jagust, W. J., Shaw, L. M., Aisen, P. S., Weiner, M. W., Petersen, R. C., & Trojanowski, J. Q. (2009). Hypothetical model of dynamic biomarkers of the Alzheimer's pathological cascade. The Lancet Neurology, 9(1), 119–128. https://doi.org/10.1016/s1474-4422(09)70299-6

[38] Jones, D. T., Kocialkowski, S., Liu, L., Pearson, D. M., BäCklund, L. M., Ichimura, K., & Collins, V. P. (2008). Tandem duplication producing a novel oncogenic BRAF fusion gene defines the majority of pilocytic astrocytomas. Cancer Research, 68(21), 8673–8677. https://doi.org/10.1158/0008-5472.can-08-2097

[39] Jones, D. T. W., Hutter, B., Jäger, N., Korshunov, A., Kool, M., Warnatz, H., Zichner, T., Lambert, S. R., Ryzhova, M., Quang, D. a. K., Fontebasso, A. M., Stütz, A. M., Hutter, S., Zuckermann, M., Sturm, D., Gronych, J., Lasitschka, B., Schmidt, S., Şeker-Cin, H., . . . Lichter, P. (2013). Recurrent somatic alterations of FGFR1 and NTRK2 in pilocytic astrocytoma. Nature Genetics, 45(8), 927–932. https://doi.org/10.1038/ng.2682

[35] Kallio, M. (1988). The incidence of intracranial gliomas in southern Finland. Acta Neurologica Scandinavica, 78(6), 480–483. https://doi.org/10.1111/j.1600-0404.1988.tb03691.x

[51] Kamnitsas, K., Ledig, C., Newcombe, V. F., Simpson, J. P., Kane, A. D., Menon, D. K., Rueckert, D., & Glocker, B. (2016). Efficient multi-scale 3D CNN with fully connected CRF for accurate brain lesion segmentation. Medical Image Analysis, 36, 61–78. https://doi.org/10.1016/j.media.2016.10.004

[59] Li, M., Liu, L., Qi, J., Qiao, Y., Zeng, H., Jiang, W., Zhu, R., Chen, F., Huang, H., & Wu, S. (2023). MRI-based machine learning models predict the malignant biological behavior of meningioma. BMC Medical Imaging, 23(1). https://doi.org/10.1186/s12880-023-01101-7

[3] Litjens, G., Kooi, T., Bejnordi, B. E., Setio, A. A. A., Ciompi, F., Ghafoorian, M., van der Laak, J. A. W. M., van Ginneken, B., & Sánchez, C. I. (2017). A Survey on Deep Learning in Medical Image Analysis. Medical Image Analysis, 42(1), 60–88. https://doi.org/10.1016/j.media.2017.07.005

[55] Louis, D. N., Perry, A., Wesseling, P., Brat, D. J., Cree, I. A., Figarella-Branger, D., Hawkins, C., Ng, H. K., Pfister, S. M., Reifenberger, G., Soffietti, R., Von Deimling, A., & Ellison, D. W. (2021). The 2021 WHO Classification of Tumors of the Central Nervous System: a summary. Neuro-Oncology, 23(8), 1231–1251. https://doi.org/10.1093/neuonc/noab106

[54] Markov random field segmentation of brain MR images. (1997, December 1). IEEE Journals & Magazine | IEEE Xplore. https://ieeexplore.ieee.org/abstract/document/650883/

[57] Menon, S. S., Guruvayoorappan, C., Sakthivel, K. M., & Rasmi, R. R. (2019). Ki-67 protein as a tumour proliferation marker. Clinica Chimica Acta, 491, 39–45. https://doi.org/10.1016/j.cca.2019.01.011

[34] Nakamura, H., Makino, K., Yano, S., & Kuratsu, J. (2011). Epidemiological study of primary intracranial tumors: a regional survey in Kumamoto prefecture in southern Japan—20-year study. International Journal of Clinical Oncology, 16(4), 314–321. https://doi.org/10.1007/s10147-010-0178-y

[6] Noor, M. B. T., Zenia, N. Z., Kaiser, M. S., Mamun, S. A., & Mahmud, M. (2020). Application of deep learning in detecting neurological disorders from magnetic resonance images: a survey on the detection of Alzheimer's disease, Parkinson's disease and schizophrenia. Brain Informatics, 7(1). https://doi.org/10.1186/s40708-020-00112-2

[58] Nowak-Choi, K., Palmer, J. D., Casey, J., Chitale, A., Kalchman, I., Buss, E., Keith, S. W., Hegarty, S. E., Curtis, M., Solomides, C., Shi, W., Judy, K., Andrews, D. W., Farrell, C., & Werner-Wasik, M. (2021). Resected WHO grade I meningioma and predictors of local control. Journal of Neuro-Oncology, 152(1), 145–151. https://doi.org/10.1007/s11060-020-03688-1

[33] Ostrom, Q. T., Gittleman, H., Liao, P., Rouse, C., Chen, Y., Dowling, J., Wolinsky, Y., Kruchko, C., & Barnholtz-Sloan, J. (2014). CBTRUS Statistical Report: Primary brain and central nervous system tumors diagnosed in the United States in 2007-2011. Neuro-Oncology, 16(suppl 4), iv1–iv63. https://doi.org/10.1093/neuonc/nou223

[13] Payan, A., & Montana, G. (2015). Predicting Alzheimer's disease: a neuroimaging study with 3D convolutional neural networks. ArXiv:1502.02506 [Cs, Stat]. https://arxiv.org/abs/1502.02506

[27] Perl, D. P. (2010). Neuropathology of Alzheimer's disease. Mount Sinai Journal of Medicine a Journal of Translational and Personalized Medicine, 77(1), 32–42. https://doi.org/10.1002/msj.20157

[37] Pfister, S., Janzarik, W. G., Remke, M., Ernst, A., Werft, W., Becker, N., Toedt, G., Wittmann, A., Kratz, C., Olbrich, H., Ahmadi, R., Thieme, B., Joos, S., Radlwimmer, B., Kulozik, A., Pietsch, T., Herold-Mende, C., Gnekow, A., Reifenberger, G., . . . Lichter, P. (2008). BRAF gene duplication constitutes a mechanism of MAPK pathway activation in low-grade astrocytomas. Journal of Clinical Investigation, 118(5), 1739–1749. https://doi.org/10.1172/jci33656

[42] Pope, W. B., Prins, R. M., Thomas, M. A., Nagarajan, R., Yen, K. E., Bittinger, M. A., Salamon, N., Chou, A. P., Yong, W. H., Soto, H., Wilson, N., Driggers, E., Jang, H. G., Su, S. M., Schenkein, D. P., Lai, A., Cloughesy, T. F., Kornblum, H. I., Wu, H., . . . Liau, L. M. (2011). Non-invasive detection of 2-hydroxyglutarate and other metabolites in IDH1 mutant glioma patients

using magnetic resonance spectroscopy. Journal of Neuro-Oncology, 107(1), 197–205. https://doi.org/10.1007/s11060-011-0737-8

[16] Prashanth, R., & Dutta Roy, S. (2018). Early detection of Parkinson's disease through patient questionnaire and predictive modelling. International Journal of Medical Informatics, 119, 75–87. https://doi.org/10.1016/j.ijmedinf.2018.09.008

[18] Prashanth, R., Dutta Roy, S., Mandal, P. K., & Ghosh, S. (2016). High-Accuracy Detection of Early Parkinson's Disease through Multimodal Features and Machine Learning. International Journal of Medical Informatics, 90, 13–21. https://doi.org/10.1016/j.ijmedinf.2016.03.001

[24] Rajan, K. B., Weuve, J., Barnes, L. L., McAninch, E. A., Wilson, R. S., & Evans, D. A. (2021). Population estimate of people with clinical Alzheimer's disease and mild cognitive impairment in the United States (2020–2060). Alzheimer S & Dementia, 17(12), 1966–1975. https://doi.org/10.1002/alz.12362

[28] Rami, L., Sala-Llonch, R., Solé-Padullés, C., Fortea, J., Olives, J., Lladó, A., Peña-Gómez, C., Balasa, M., Bosch, B., Antonell, A., Sanchez-Valle, R., Bartrés-Faz, D., & Molinuevo, J. L. (2012). Distinct functional activity of the precuneus and posterior cingulate cortex during encoding in the preclinical stage of Alzheimer's disease. Journal of Alzheimer S Disease, 31(3), 517–526. https://doi.org/10.3233/jad-2012-120223

[8] Sarraf, S., & Tofighi, G. (2016). Classification of Alzheimer's Disease using fMRI Data and Deep Learning Convolutional Neural Networks. ArXiv:1603.08631 [Cs]. https://arxiv.org/abs/1603.08631

[14] Sarraf, S., DeSouza, D. D., Anderson, J., & Tofighi, G. (2016). DeepAD: Alzheimer's Disease Classification via Deep Convolutional Neural Networks using MRI and fMRI. https://doi.org/10.1101/070441

[21] Selkoe, D. J. (2011). Resolving controversies on the path to Alzheimer's therapeutics. Nature Medicine, 17(9), 1060–1065. https://doi.org/10.1038/nm.2460

[47] Shah, G. D., Kesari, S., Xu, R., Batchelor, T. T., O'Neill, A. M., Hochberg, F. H., Levy, B., Bradshaw, J., & Wen, P. Y. (2006). Comparison of linear and volumetric criteria in assessing tumor response in adult high-grade gliomas1. Neuro-Oncology, 8(1), 38–46. https://doi.org/10.1215/s1522851705000529

[7] Shatte, A. B. R., Hutchinson, D. M., & Teague, S. J. (2019). Machine learning in mental health: a scoping review of methods and applications. Psychological Medicine, 49(09), 1426–1448. https://doi.org/10.1017/s0033291719000151

[16] Smith-Bindman, R., Miglioretti, D. L., Johnson, E., Lee, C., Feigelson, H. S., Flynn, M., Greenlee, R. T., Kruger, R. L., Hornbrook, M. C., Roblin, D., Solberg, L. I., Vanneman, N.,

Weinmann, S., & Williams, A. E. (2012). Use of Diagnostic Imaging Studies and Associated Radiation Exposure for Patients Enrolled in Large Integrated Health Care Systems, 1996-2010. JAMA, 307(22).

[64] Subramoniam, M., R, A. T., R, A. P., & G, S. K. (2021b). Deep learning based prediction of Alzheimer's disease from magnetic resonance images. arXiv (Cornell University). https://doi.org/10.48550/arxiv.2101.04961

[49] The Multimodal Brain Tumor Image Segmentation Benchmark (BRATS). (2015, October 1). IEEE Journals & Magazine | IEEE Xplore. https://ieeexplore.ieee.org/abstract/document/6975210/

[53] Tustison, N. J., Shrinidhi, K. L., Wintermark, M., Durst, C. R., Kandel, B. M., Gee, J. C., Grossman, M. C., & Avants, B. B. (2014). Optimal Symmetric Multimodal Templates and Concatenated Random Forests for Supervised Brain Tumor Segmentation (Simplified) with ANTsR. Neuroinformatics, 13(2), 209–225. https://doi.org/10.1007/s12021-014-9245-2

[61] Van Griethuysen, J. J., Fedorov, A., Parmar, C., Hosny, A., Aucoin, N., Narayan, V., Beets-Tan, R. G., Fillion-Robin, J., Pieper, S., & Aerts, H. J. (2017). Computational Radiomics system to decode the radiographic phenotype. Cancer Research, 77(21), e104–e107. https://doi.org/10.1158/0008-5472.can-17-0339

[46] Wen, P. Y., Chang, S. M., Van Den Bent, M. J., Vogelbaum, M. A., Macdonald, D. R., & Lee, E. Q. (2017). Response assessment in Neuro-Oncology clinical trials. Journal of Clinical Oncology, 35(21), 2439–2449. https://doi.org/10.1200/jco.2017.72.7511

[26] Wimo, A., Ali, G., Guerchet, M., Prince, M., Prina, M., & Wu, Y. (2015, September 21). World Alzheimer Report 2015: The global impact of dementia: An analysis of prevalence, incidence, cost and trends. ADI - World Alzheimer Report 2015. https://www.alzint.org/resource/world-alzheimer-report-2015/

[60] Woznicki, P., Laqua, F., Bley, T., & Baeßler, B. (2022). AutoRadiomics: a framework for reproducible radiomics research. Frontiers in Radiology, 2. https://doi.org/10.3389/fradi.2022.919133

[12] YİĞİT, A., & IŞIK, Z. (2020). Applying deep learning models to structural MRI for stage prediction of Alzheimer's disease. TURKISH JOURNAL of ELECTRICAL ENGINEERING & COMPUTER SCIENCES, 28(1), 196–210. https://doi.org/10.3906/elk-1904-172

[36] Yunoue, S., Tokuo, H., Fukunaga, K., Feng, L., Ozawa, T., Nishi, T., Kikuchi, A., Hattori, S., Kuratsu, J., Saya, H., & Araki, N. (2003). Neurofibromatosis Type I Tumor Suppressor Neurofibromin Regulates Neuronal Differentiation via Its GTPase-activating Protein Function toward Ras. Journal of Biological Chemistry, 278(29), 26958–26969. https://doi.org/10.1074/jbc.m209413200

[63] Zhang, S., Richter, J., Veale, J., Phan, V. M. H., Candy, N., Poonnoose, S., Agzarian, M., & To, M. (2025). Development of Hybrid radiomic Machine learning models for preoperative prediction of meningioma grade on multiparametric MRI. PubMed, 135, 111118. https://doi.org/10.1016/j.jocn.2025.111118

[29] Zhou, J., Greicius, M. D., Gennatas, E. D., Growdon, M. E., Jang, J. Y., Rabinovici, G. D., Kramer, J. H., Weiner, M., Miller, B. L., & Seeley, W. W. (2010). Divergent network connectivity changes in behavioural variant frontotemporal dementia and Alzheimer's disease. Brain, 133(5), 1352–1367. https://doi.org/10.1093/brain/awq075

[17] Sharma, S., Moon, C. S., Khogali, A., Haidous, A., Chabenne, A., Ojo, C., Jelebinkov, M., Kurdi, Y., & Ebadi, M. (2013). Biomarkers in Parkinson's disease (recent update). Neurochemistry International, 63(3), 201–229. https://doi.org/10.1016/j.neuint.2013.06.005

APPENDICES

The following appendix contains the techniques and fundamental programming elements which enabled MRI classification through deep learning methods in this research. Authors have published the program source codes along with complete documentation in their supplementary materials that accompany this thesis.

1. Overview

The classification pipeline utilized PyTorch together with EfficientNet-B2 for its development. The system follows a data-preprocessing phase and a training process using 5-fold cross-validation that is followed by an inference stage. The automatic script analyzes five types of medical images which include Demented, NonDemented, Glioma, Meningioma and NoTumor.

2. Folder Structure

```
Dataset/
├── train/
│   ├── Demented/
│   ├── NonDemented/
│   ├── Glioma/
│   ├── Meningioma/
│   └── NoTumor/
└── test/
    ├── Demented/
    ├── NonDemented/
    ├── Glioma/
    ├── Meningioma/
    └── NoTumor/
```

3. Key Scripts and Functions

MRIDataset – Custom PyTorch Dataset class

get_efficientnet_b2() – Loads the modified EfficientNet-B2 model

train_one_epoch() and validate_one_epoch() – Training and validation loops

run_kfold() – Performs 5-fold cross-validation

inference() – Performs inference on the test set

4. Example Hyperparameters

NUM_CLASSES = 5
NUM_EPOCHS = 15
BATCH_SIZE = 16
K_FOLDS = 5
LR = 0.0005

5. Sample Training Command

python classification.py

6. Sample Inference Command

python inference.py

7. Source Code Location

All code files are provided in the digital supplementary materials as a .zip package titled: **"MRI_Classification_Code_Package.zip"**